XL CILAMCE
IBERO-LATIN AMERICAN CONGRESS ON COMPUTATIONAL METHODS IN ENGINEERING
NOVEMBER 11-14, 2019
Praiamar Natal Hotel & Convention
Natal, RN-BRAZIL

VERTICAL AXIS WIND TURBINE WAKE FLOW ASSESSMENT USING OPENFOAM

Hugo G. Castro
guillermo.castro@conicet.gov.ar
Laboratorio de Mecánica Computacional (LAMeC-FI-UNNE-IMIT) - CONICET - GIMeF (UTN FRRe)
Av. Las Heras 727, 3500, Resistencia, Chaco, Argentina
Javier L. Mroginski
Juan M. Podestá
javierm@ing.unne.edu.ar
jmapodesta@gmail.com
Laboratorio de Mecánica Computacional (LAMeC-FI-UNNE-IMIT) - CONICET
Av. Las Heras 727, 3500, Resistencia, Chaco, Argentina

Abstract.

Wind power is one of the means of producing renewable energy that has grown in popularity due to the horizontal axis wind turbine great efficiency. However, vertical axis wind turbines (VAWTs) are becoming an interesting option in urban environments. As it is well known, the wake flow generated by the kinetic energy extraction of the wind turbine blades has a direct influence on the wind turbine performance, whether isolated or grouped in a wind farm. This work presents a computational fluid dynamics (CFD) study of a Darrieus VAWT wake flow. The wind turbine is assumed to be located inside a boundary-layer wind tunnel with different inflow conditions. The complete coupling between the rotating rigid solid and the fuid flow is implemented by open source CFD OpenFOAM software. Three dimensional unsteady flow simulations are carried out by means of the Unsteady Reynolds Averaged Navier-Stokes (URANS) method and using the sliding mesh technique in order to explicity resolved the turbine rotation. The obtained results are compared with previous experimental work, showing a good agreement.

Keywords: Vertical Axis Wind Turbine, wake flow, Computational Fluid Dynamics

1 Introduction

Due to its sustainability and geographically wide availability, wind energy has received increasing attention in recent years. Compared to horizontal axis wind turbines (HAWTs), vertical-axis wind turbines (VAWTs) are smaller and more easily located within cities. Furhtermore, these later turbines produce electrical energy even at low wind velocities and are easier to manufacture [1, 2]. Nevertheless, relatively low aerodynamic efficiency and high cost are two major problems of VAWTs, requiring the development of advanced methods/models to improve their performance and minimise costs.

Wind turbines, whatever its classification be, are exposed to the atmospheric turbulence. This unsteady velocity field interacts directly with the blades, producing vorticy in its wake. Besides, it is well know that the aerodynamics of VAWTs are more complex than of HAWTs, given that lift and drag vary continuously in a cycle as the relative angle of attack changes. These characteristics make the analysis of VAWTs a very challenging and interesting field of study.

There are several studies attempting to clarify different aspects of the VAWT aerodynamics. Balduzzi et al. [3] presented an extensive analysis on the main parameters in order to obtain the most effective settings for a two-dimensional computational simulation of an H-type Darrieus turbine. It was found that in Darrieus wind turbines, the incidence angle varies constantly with the azimuthal position of the blade, leading to a strong interaction between both halves of the rotor (upwind and downwind).

Moreover, despite the importance that inflow turbulence has on wind turbine performance, its study is less common than other effects on wind turbines. Precisely this point was observed and addressed by Hohman et al. [4]. In their work, the authors analyzed the relationship between the inflow turbulence and the wake structure recovery by testing in a wind tunnel a VAWT model.

In this work, the Open Source Field Operation and Manipulation (OpenFOAM) C++ library is used to model computationally a three-dimensional VAWT. In order to evaluate the OpenFOAM capabilities to realistically reproduce the wake behind the wind turbine blades using the unsteady Reynolds averaged Navier-Stokes (URANS) model, the numerical results are compared with the experimental measurements obtained by Hohman et al. [4].

2 Description of the study case

The aim of this work is to study and to analyze, using CFD simulations, the experimental setup presented in Figure (1), reproduced from the work of Hohman et al. [4]. The experiments were performed using a standard recirculating type wind tunnel with a constant flow speed of 8.5m/s.

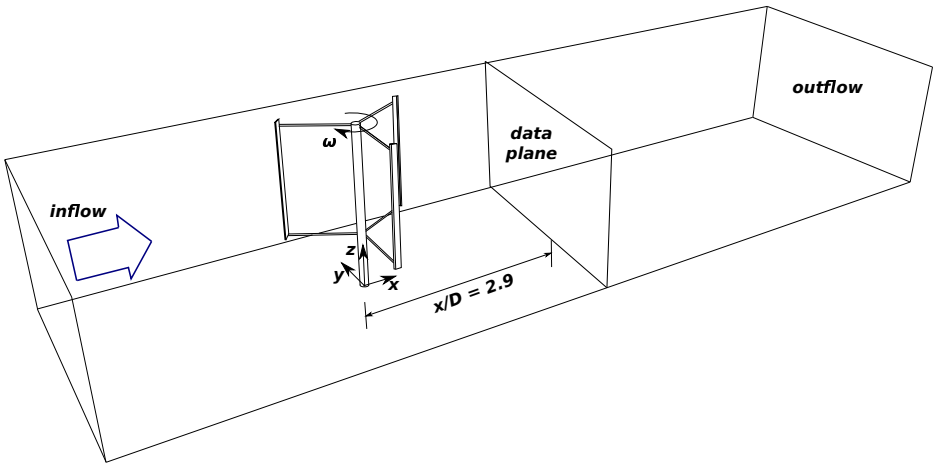

Figure 1. Experimental setup by Hohman et al. [4].

The origin of the coordinate system is defined at intersection of the wind turbine axis of rotation with the wind tunnel floor. The turbine diameter D is approximately equivalent to 10 chord lengths,

c. Three straight NACA 0020 blades were part of the design, giving a solidity of $\sigma = 0.3$. Table 1 summarizes the rotor geometrical design.

Blades number (n)	3
Blades shape	straight
Blades airfoil	NACA0020
Diameter of the turbine (D)	0.4064 m
Chord (c)	0.0406 m
Blade height (h)	0.2794 m

Table 1. Geometrical characteristics of the rotor [4].

The experiments were conducted with a turbine Reynolds number Re_t given by:

$$Re_t = \frac{U_\infty D}{\nu} = \frac{8.5 \times 0.4064}{1.45 \times 10^{-5}} \approx 2.38 \times 10^5 \tag{1}$$

being U_∞ the inflow velocity and $\nu = 1.45 \times 10^{-5}$ m^2/s the kinematic viscosity of air. Another important quantity that is commonly used in the study of VAWTs is the tip speed ratio, λ, here defined as

$$\lambda = \frac{\omega D}{2U_\infty} \tag{2}$$

where ω is the angular velocity. In the experiments reported by Hohman et al. [4], two values of tip speed ratio were used, $\lambda = 1$ and $\lambda = 3$. Considering that the inflow velocity was kept constant at $U_\infty = 8.5$ m/s, the angular velocities were $\omega = 41.83$ rad/s and $\omega = 125.49$ rad/s. In this work, only the lower angular velocity were taken into account, in order to reduce the computational cost of the simulation. Accordingly, the blade Reynolds number Re_b resulted in:

$$Re_b = \frac{c\, D\, \omega}{2\nu} = \frac{0.0406 \times 0.0406 \times 41.83}{2 \times 1.45 \times 10^{-5}} \approx 2.38 \times 10^4 \tag{3}$$

In the experimental test, the constant rotation of the turbine was achieved by a motor located downstream of the model and inside the wind tunnel section. Hohman et al. [4] opted for a constant rate of rotation against a self-spinning turbine concept based on previous works, which suggested that both approaches could produce similar wake structures at similar Reynolds number, see for example the work of Araya and Dabiri [5].

3 Numerical setup

3.1 Turbulence modeling

The unsteady flow around the VAWT is modeled by the unsteady Reynolds-averaged Navier-Stokes equations (URANS) using the turbulence shear stress transport (SST) $k-\omega$ model for closure. According to Balduzzi et al. [3], the SST $k-\omega$ model shows a better performance in terms of stability and reliability compared to other models as well as the best agreement with experiments. This is related to the fact that SST $k-\omega$ performs well into boundary layers even with pressure separation. Furthermore, is not as sensitive as the $k-\omega$ model with respect to inlet boundary conditions.

The SST $k-\omega$ approach is a two equation model for the turbulence kinetic energy, k, and the turbulence specific dissipation rate, ω. The turbulence kinetic energy equation is given by

$$\frac{\partial \rho k}{\partial t} + \frac{\partial \rho U_j k}{\partial x_j} = \tilde{P}_k - \beta^* \rho \omega k + \frac{\partial}{\partial x_j}(\Gamma_k \frac{\partial k}{\partial x_j}) \tag{4}$$

whereas the turbulence specific dissipation rate equation by

$$\frac{\partial \rho\omega}{\partial t} + \frac{\partial \rho U_j \omega}{\partial x_j} = \frac{\gamma}{\nu_t} P_k - \beta\rho\omega^2 + \frac{\partial}{\partial x_j}(\Gamma_k \frac{\partial \omega}{\partial x_j}) + (1 - F_1) 2\rho\sigma_{\omega^2} \frac{1}{\omega} \frac{\partial k}{\partial x_j} \frac{\partial \omega}{\partial x_j}. \tag{5}$$

where

$$\begin{aligned} \Gamma_k &= \mu + \mu_t \sigma_k \\ \Gamma_\omega &= \mu + \mu_t \sigma_\omega \\ P_k &= \tau_{ij} \frac{\partial U_i}{\partial x_j} \\ \tilde{P}_k &= min(P_k; c_1\epsilon) \\ \mu_t = \rho \cdot \nu_t &= \rho \cdot \frac{a_1 k}{max(a_1\omega; S \cdot F_2)} \end{aligned} \tag{6}$$

The blending function F_1 is defined as

$$F_1 = \tanh\left(\left(min\left[max\left(\frac{\sqrt{k}}{\beta^*\omega y}, \frac{500\nu}{y^2\omega}\right), \frac{4\rho\sigma_{\omega^2} k}{CD_{k\omega} y^2}\right]\right)^4\right) \tag{7}$$

being y the distance to the nearest wall and

$$CD_{k\omega} = max\left(2\rho\sigma_{\omega^2} \frac{1}{\omega} \frac{\partial k}{\partial x_j} \frac{\partial \omega}{\partial x_j}, 10^{-10}\right), \tag{8}$$

while the second blending function F_2 is

$$F_2 = \tanh\left(\left(max\left[\frac{2\sqrt{k}}{\beta^*\omega y}, \frac{500\nu}{y^2\omega}\right]\right)^2\right). \tag{9}$$

All the constants in the model are computed from the corresponding constants for the $k - \epsilon$ and $k - \omega$ models using a blending function $\phi = \phi_1 F_1 + \phi_2(1 - F_1)$ where ϕ_1 stands for the coefficients of the $k - \epsilon$ model and ϕ_2 for the coefficients of the $k - \omega$ model.

OpenFOAM uses the finite volume method and provides three methods to handle the pressure-velocity coupling for solving the discretized form of the Navier-Stokes equations: PISO (pressure implicit with split operator); SIMPLE (semi-implicit method for pressure linked equations) and PIMPLE (merged PISO-SIMPLE). This study uses the solver `pimpleFoam`, which is based on the PIMPLE algorithm, enforced a maximum convective CFL$= 1$. This algorithm enables more robust results when adopting different meshes and timesteps [6].

In order to reduce the computational costs, PIMPLE algorithm is used with one corrector, 2 outer correctors and no non-orthogonal correctors. Time-dependent term is discretized using a first-order Euler approximation. For the spatial discretization, a central second-order differential scheme is used for the advective terms and a 2nd order bounded scheme for the diffusive terms.

3.2 Boundary conditions

The dimensions of the computational domain adopted in this work are: W = 0.91 m width (normal or lateral direction Y), H = 0.61 m tall (vertical direction Z) and $15D$ = 6.096 m depth (longitudinal direction X, following the flow direction), Fig. 2. These geometric dimensions are in agreement with the main dimensions of the wind tunnel test section.

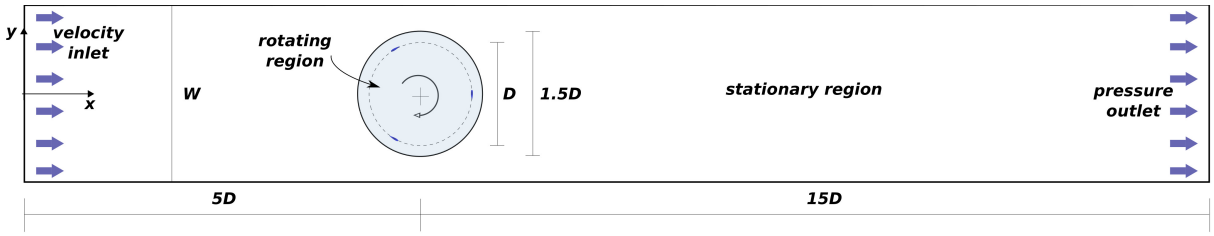

Figure 2. Basic configuration of the computational domain (top view).

The boundaries of the computational domain can be divided into *inlet*, *outlet*, *lateral walls*, *roof*, *floor* and *AMI interface*, as shown in Fig. 3. The slip boundary condition is applied on the roof and lateral walls, while no-slip condition is applied on the floor. To take into account the imposed rotational movement, the boundary condition `movingWallVelocity` is applied on the blades. This condition corrects fluxes for moving boundaries, behaving exactly as a no-slip condition when a wall do not move.

The sliding interface capability is implementing in this work by using a Cyclic Arbitrary Mesh Interface (AMI). This feature enable the simulation across disconnected, adjacent, mesh domains [7]. The sliding interface is used to connect the rotating and stationary regions, as shown in Fig. 2 and Fig. 3.

To prescribe boundary conditions for ω and k, wall functions `omegaWallFunction` which ensures continuous near-wall behaviour for all y^+, and `kqRWallFunction` are used, respectively. This later function applies a zero-gradient condition between the wall and the first element for the modeled value of k [6]. At the outlet boundary, null pressure is set. All boundary conditions for the analyzed case are summarized in Table 2, according to the OpenFOAM convention and in correspondence with Fig. 3.

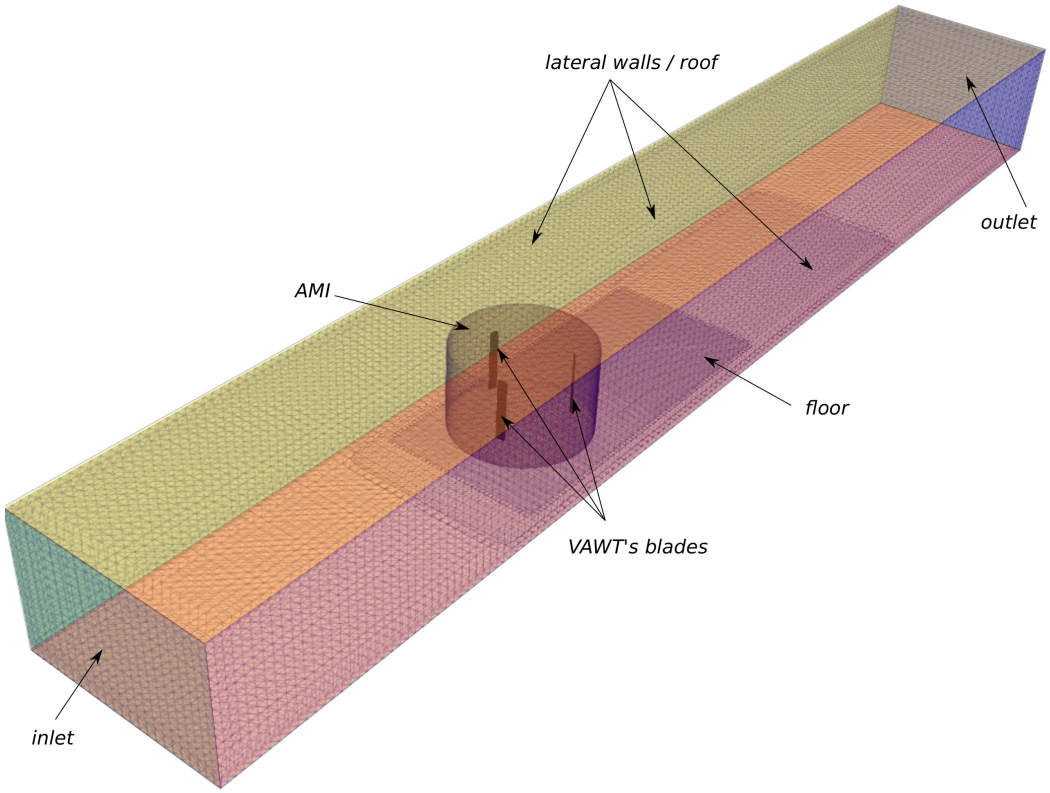

Figure 3. Three-dimensional computational domain.

Table 2. Boundary conditions.

	density-normalized presure (m^2/sec^2)	velocity (m/sec)	nut (m^2/sec)
inlet	`zeroGradient`	`fixedValue uniform (8.5 0 0)`	`calculated uniform 0`
outlet	`fixedValue uniform 0`	`inletOutlet inletValue uniform (0 0 0) value $internalField`	`calculated uniform 0`
floor	`zeroGradient`	`noSlip`	`nutkWallFunction`
VAWT blades	`zeroGradient`	`movingWallVelocity uniform (0 0 0)`	`nutkWallFunction`
roof and lateral walls	`slip`	`slip`	`calculated uniform 0`

3.3 Computational mesh

The experimental results employed for comparison were obtained in a wind tunnel with a test section measuring $0.61m$ high by $0.91m$ wide [4]. Thus, in order to accurately represent the experimental test, a computational grid composed by 3.2 million (M) cells (roughly 3.0 M hexahedra), approximately. To achieve a good quality mesh that accurately captures the turbulence scales that influence on the interactions of the model immersed in the turbulent flow, the mesh is composed by different refinement box zones as it can be seen in Fig. 3 and Fig. 4.

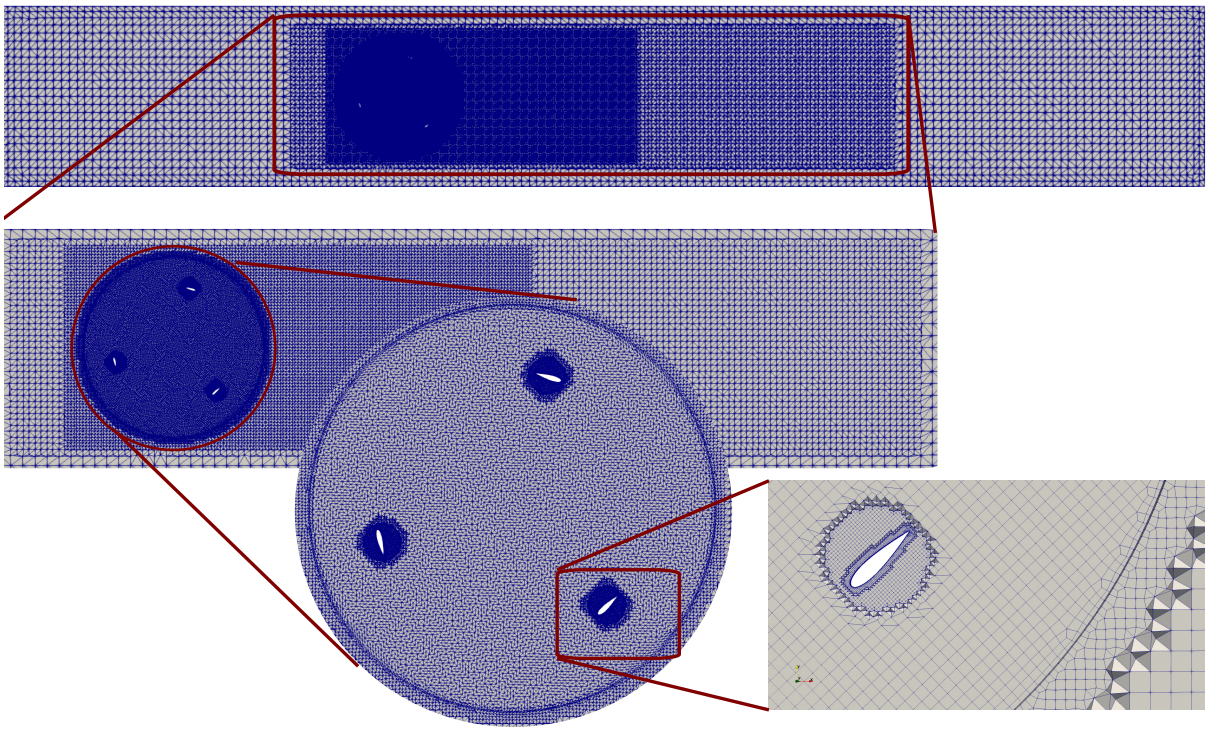

Figure 4. Detail of the mesh.

4 Results

In this section, the obtained numerical results are compared against de experimental data. The comparison is made by examining the differences in the mean and fluctuating velocities in different planes on the wake.

The profiles of U and $\overline{u^2}$ are shown in Figs 5 and 6. These profiles follow the three-dimensional and asymmetric wake structure in the most part of them. In these figures it is very clear the difference in the streamwise variance, exactly at $y/D = 0$. This deficit can be partially explained by the lack of a rotor shaft in the numerical simulation. The presence of this cylinder in the computational domain will detract some energy from the flow.

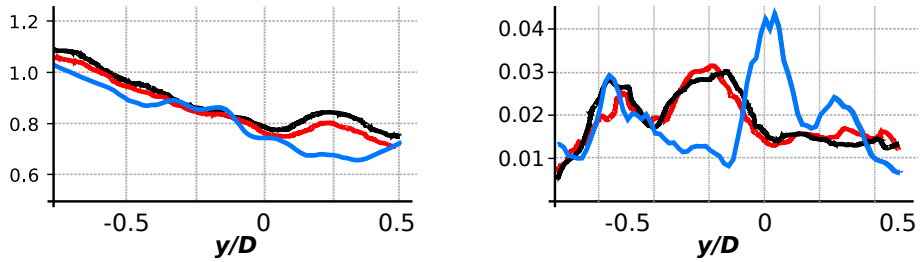

Figure 5. Plane $z/\delta = 0.73$ - *Left.:* streamwise velocity U/U_∞. *Right.:* streamwise variance $\overline{u^2}/U_\infty^2$. Color reference - black/red: experimental test - blue: computational simulation.

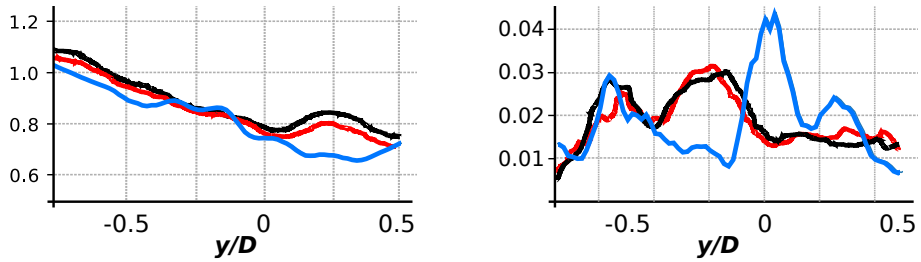

Figure 6. Plane $z/\delta = 0.55$ - *Left.:* streamwise velocity U/U_∞. *Right.:* streamwise variance $\overline{u^2}/U_\infty^2$. Color reference - black/red: experimental test - blue: computational simulation.

5 Conclusions

In the present work, a computational simulation of an experimental test of a VAWT were implemented and validated. The simulation was performed using the OpenFOAM software in its version $v1812$. This version provides several tools suitable for the study of turbomachinery, such as cyclic Arbitrary Mesh Interface (AMI) with functions to compute AMI patches performance, mesh movements as a solid body (without deformations), turbulence models like $k-\omega\ SST$, among other features.

Despite some differences in the velocities in the wake, it can be noted that the computational simulation represent adequately the main behavior of the turbulent flow. As the results are in good agreement with the experimental data, it is possile to conclude that the numerical methods provided by OpenFOAM are accurate enough to reproduce the turbulent flow behind wind turbines.

Acknowledgements

This research was partially funded by Consejo Nacional de Investigaciones Cienífícas y Técnicas (CONICET, Argentina), Secretaría de Ciencia y Tecnología de la Universidad Tecnológica Nacional Facultad Regional Resistencia (UTN-FRRe, Argentina, Grant PID 2018 ENUTIRE0004912TC), Universidad Nacional del Nordeste, Facultad de Ingenierá (UNNE, Argentina, Grant PID 2018 17D005). Also,

the authors would like to acknowledge the financial support from the Agencia Nacional de Promoción Científica y Tecnológica (ANPCyT, Argentina, Grant PICT 2015 IB CONICET 2739).

References

[1] Kaldellis, J. K. & Zafirakis, D., 2011. The wind energy (r)evolution: A short review of a long history. *Renewable Energy*, vol. 36, n. 7, pp. 1887 – 1901.

[2] Sobhani, E., Ghaffari, M., & Maghrebi, M. J., 2017. Numerical investigation of dimple effects on darrieus vertical axis wind turbine. *Energy*, vol. 133, pp. 231 – 241.

[3] Balduzzi, F., Bianchini, A., Maleci, R., Ferrara, G., & Ferrari, L., 2016. Critical issues in the CFD simulation of darrieus wind turbines. *Renewable Energy*, vol. 85, pp. 419 – 435.

[4] Hohman, T., Martinelli, L., & Smits, A., 2018. The effects of inflow conditions on vertical axis wind turbine wake structure and performance. *Journal of Wind Engineering and Industrial Aerodynamics*, vol. 183, pp. 1–18.

[5] Araya, D. & Dabiri, J., 2015. A comparison of wake measurements in motor-driven and flow-driven turbine experiments. *Experiments in Fluids*, vol. 56:150.

[6] Robertson, E., Choudhury, V., Bhushan, S., & Walters, D., 2015. Validation of OpenFOAM numerical methods and turbulence models for incompressible bluff body flows. *Computers & Fluids*, vol. 123, pp. 122–145.

[7] OpenCFD, 2016. *OpenFOAM - The Open Source CFD Toolbox - User's Guide*. OpenCFD Ltd., United Kingdom, 4.0 edition.